

Accepted Manuscript

Application of fractal models to characterization of vertical distribution of geochemical element concentration

Renguang Zuo, Qiuming Cheng, Qinglin Xia

PII: S0375-6742(08)00141-6
DOI: doi: [10.1016/j.gexplo.2008.11.020](https://doi.org/10.1016/j.gexplo.2008.11.020)
Reference: GEXPLO 4583

To appear in: *Journal of Geochemical Exploration*

Received date: 8 August 2008
Accepted date: 17 November 2008



Please cite this article as: Zuo, Renguang, Cheng, Qiuming, Xia, Qinglin, Application of fractal models to characterization of vertical distribution of geochemical element concentration, *Journal of Geochemical Exploration* (2008), doi: [10.1016/j.gexplo.2008.11.020](https://doi.org/10.1016/j.gexplo.2008.11.020)

This is a PDF file of an unedited manuscript that has been accepted for publication. As a service to our customers we are providing this early version of the manuscript. The manuscript will undergo copyediting, typesetting, and review of the resulting proof before it is published in its final form. Please note that during the production process errors may be discovered which could affect the content, and all legal disclaimers that apply to the journal pertain.

22 indicating that Qulong copper deposit has a good continuity of mineralization.

23 *Keywords:* Fractal; Box dimension; Power-law frequency; Hurst exponent; Borehole; Qulong

24 **1. Introduction**

25 Characterization of the distribution of geochemical elements in boreholes is of significance to evaluate
26 the quality and quantity of mineral resources in the mining industry. In the past several decades, the nature
27 of the distributions of geochemical elements in rocks has been intensively studied in order to discover a
28 universal geochemical law. Ahrens(1954, 1963a, 1963b, 1966) proposed that the frequency distributions of
29 most minor and trace elements in rocks and ore deposits were positively skewed and could be satisfactorily
30 described by the lognormal law; while the distribution of major elements is more complex. For example,
31 the silica distribution of surface rocks where there are basic and acid maxima (Richardson, 1923) exhibits
32 multimodal distributions (Allègre and Lewin, 1995). The distributions of geochemical elements in
33 boreholes also exhibit power-law characteristics, which can be fitted by fractal models (Sanderson et al.,
34 1994; Monecke et al, 2001).

35 A fractal is defined as a set in which the Hausdorff dimension strictly exceeds the topological
36 dimension (Mandelbrot, 1983). It has generally the following features: (1) It has a fine structure at
37 arbitrarily small scales: (2) It is too irregular to be easily described in traditional Euclidean geometric
38 language; (3) It is self-similar; (4) It has a Hausdorff dimension which is greater than its topological
39 dimension, and (5) It has a simple and recursive definition (Kenneth,1997). Fractal models have been
40 extensively applied to physical and chemical quantities with geometrical support in the past two decades. In
41 geology, this approach has been used for characterizing geological objects and geological features
42 (Mandelbrot, 1983; Cheng, 1995; Wang et al., 2006; Wang et al., 2008) and for separating anomalies from
43 background values (Cheng et al., 1994; Cheng et al., 2000), and for quantifying properties of mineralization

44 and mineral deposits (Turcotte, 1996, 2002; Sanderson et al., 1994; Agterberg et al., 1993; Li et al., 1994;
 45 Shi and Wang, 1998). In this paper, the fractal dimensions including box dimension, power-law frequency
 46 and Hurst exponents were utilized to characterize the vertical distribution of trace elements and to evaluate
 47 the mineralized continuity based on borehole datasets. For demonstration purposes, a case from Qulong
 48 Copper Deposit will be studied. In the next section, the box dimension, power-law frequency model and
 49 Hurst exponent are briefly introduced for demonstrating how to process data.

50 **2. Fractal Models**

51 *2.1. Box Counting Method and Box Dimensions*

52 Box counting is one of most popular methods to estimate the fractal dimensions. It can be used for
 53 measurement of the irregularity of patterns, and can be implemented with the aid of GIS. A group of grids
 54 with box size “ δ ” were used to cover the concentration curve vector layers, and these grids were used for
 55 counting the corresponding number of grey boxes ($N(\delta)$) occupied by grade curves. Data pairs for box
 56 size δ and number N can be plotted on a log–log paper and linear regression applied to fit a straight line
 57 from which the box dimension D can be estimated. The box-counting method results in a power-law
 58 relation:

$$59 \quad N(\delta) \propto \delta^{-D} \quad (1)$$

60 It can be rewritten as

$$61 \quad \text{Log}[N(\delta)] = C - D\text{Log}(\delta) \quad (2)$$

62 where $N(\delta)$ is the number of cells containing grade curves, C is a constant, and D is the box dimension.

63 *2.2. Power-law Frequency Model*

64 The power-law frequency model was used to measure the frequency distribution of element
 65 concentration. This model has been demonstrated by many studies (Turcotte, 1996; Sanderson et al., 1994;

66 Li et al., 1994; Shi and Wang, 1998), and can be expressed as

$$67 \quad N(\geq c) \propto c^{-D} \quad (3)$$

68 It also can be rewritten as

$$69 \quad \text{Log}[N(\geq c)] = C - D\text{Log}(c) \quad (4)$$

70 where $N(\geq c)$ is the number of samples with a content greater than c , C is a constant and D is the fractal
71 dimension.

72 2.3. Hurst Exponent

73 The Hurst Exponent proposed by Hurst (1951) is directly related to the fractal dimension of a process,
74 which gives a measure of the process roughness. The Hurst exponent, H , is a self-similarity parameter
75 which measures the long-range dependence in a time series, and provides a measure of long-term
76 nonlinearity. The expected values of H lie between 0 and 1. For $H = 0.5$, the cumulative behavior is a
77 random walk and the process produces uncorrelated white noise. $H < 0.5$ represents anti-persistent behavior
78 and $H > 0.5$ is fractional Brownian motion with increasing persistence strength as H approaches 1.

79 The rescaled range statistic (R/S) analysis can be used to estimate the Hurst exponent (Mandelbrot and
80 Wallis, 1969), which can be described as follows: The ordered data sequence is divided into d contiguous
81 sub-series of length n , where $d \times n = N$, the total number of the samples. For each of these sub-series m ,
82 where $m = 1, \dots, d$.

83 (1) Determine the mean, E_m , of each sub-series.

84 (2) Determine the standard deviation, S_m , of each sub-series.

85 (3) Normalize the data ($Z_{i,m}$) by subtracting the mean from each data point:

$$86 \quad X_{i,m} = Z_{i,m} - E_m \quad m = 1, 2, \dots, n \quad (5)$$

87 (4) Use the normalized data creating a cumulative series by consecutively summing the data points:

$$88 \quad Y_{i,m} = \sum_{j=1}^i X_{j,m} \quad i = 1, 2, \Lambda, n \quad (6)$$

89 (5) Use the new cumulative series to find the range by subtracting the minimum value from the
90 maximum value:

$$91 \quad R_m = \max\{Y_{1,m}, \Lambda, Y_{n,m}\} - \min\{Y_{1,m}, \Lambda, Y_{n,m}\} \quad (7)$$

92 (6) Rescale the range, R_m / S_m by dividing the range based on the standard deviation.

93 (7) Calculate the mean of the rescaled range for all sub-series of length n :

$$94 \quad (R/S)_n = \frac{1}{d} \sum_{i=1}^d R_m / S_m \quad (8)$$

95 (8) The length of n must be increased to the next higher value, where $d \times n = N$, and d is an integer
96 value. Step 1 to 7 are then repeated, these steps should be repeated until $n = N / 2$.

97 (9) Finally, the value of H is estimated from the slope of the regression line with $\log(n)$ versus
98 $\log(R/S)$.

99 **3 Geological Setting and Sampling**

100 The study area, Qulong Copper Deposit, is a large porphyry copper deposit in the Gangdese porphyry
101 copper belt, located approximately 110km southeast of Lhasa, the capital city of Xizang (Tibet), western
102 China. A simplified geological map is shown in Fig.1. The host rocks are biotite-adamellite ($\beta\eta\gamma$)
103 covering approximately 60% of the middle and east part of the district, and adamellite quartz porphyry
104 ($\eta\lambda\pi$) located in the northwest zone. Figure 2 shows the profile of the eighth exploring line where the
105 rocks mainly consist of quartz, biotite-adamellite granites ($\beta\eta\gamma$) and orebodies. The geological features of
106 the Qulong deposit were studied in detail by Rui et al. (2003) and Zheng et al. (2002). The Qulong copper
107 deposit consists of 7 orebodies, CuI, CuII, CuIII, CuIV, CuV, CuVI, and CuVII, among which CuII, the
108 largest one, occurs in the northwest, and CuVI, the smallest one, occurs in the central part of the zone. 10

109 Cu mineralized datasets and 1 non-mineralized dataset, ZK1901, were obtained by continuous sampling
110 every 2m and 7m along borehole in the zone, respectively. The properties and statistical results of the
111 boreholes datasets are summarized in Table 1, and the line graphs of Cu values from mineralized boreholes
112 are shown in Fig.3.

113 4. Results and discussions

114 4.1. Frequency distribution of Cu

115 The property of frequency distributions of element concentration are usually evaluated in histograms
116 that display arbitrarily chosen, linearly scaled concentration intervals on the abscissa and the frequency of
117 individual analyses whose results fall in a particular class interval on the ordinate. The histograms (Fig. 4)
118 show that the distributions of Cu values in the mineralized borehole are positively skewed.

119 4.2. Box Dimensions

120 The box dimensions can be obtained from the line graphs of Cu (Fig. 3). The Cu values lines can be
121 converted from a vector to a raster. Different appropriate cell sizes can be used to determine the count of
122 cells. Then a log-log plot of cell size versus count made in Excel with a trend line using a power function
123 and providing the coefficient of determination, R^2 , will provide the fractal dimensions and coefficient of
124 explanation. The log-log plots of cell size versus count are shown in Fig. 5 and Fig. 8B, and the box
125 dimensions and R^2 are listed in Table 2. The results show that the vertical distribution of Cu in mineralized
126 boreholes exhibits self-similarity and box dimensions range from 1.28 to 1.37, with R^2 greater than 0.99,
127 indicating that the vertical distributions of Cu have approximate irregularity. The results also demonstrate
128 that the box dimensions of mineralized boreholes are greater than or equal to that of the distribution of Cu
129 in the non-mineralized borehole, indicating that the mineralization makes the vertical distribution of Cu
130 values more irregular.

131 *4.3. Power-law Frequency Distribution of Cu Values*

132 The results obtained by the power-law frequency model for mineralized boreholes are shown in Fig.6
133 and listed in the middle of Table 2. The log-log plots of cumulative number versus Cu values show the
134 distribution of Cu in the mineralized boreholes satisfying bifractal. The two portions of the plot define a
135 crossover point at 0.33 (Table 2), for Cu values less than and greater than 0.33, fractal dimensions range
136 from 0.1 to 0.65, in the non-mineralized rocks, and range from 2.71 to 5.79, in the mineralized rocks.

137 Larger fractal dimensions of mineralization imply more homogeneous mineralization. It can be
138 explained that fractal dimensions are estimated from the frequency of Cu values and can reflect the
139 proportion of Cu values. Larger fractal dimension implies less numbers of Cu values greater than a specific
140 Cu value. It means that the Cu value change slowly along the borehole, indicating more homogeneous
141 mineralization. The coefficient of variation (CV), which is equal to the standard deviation divided by the
142 average, identifies the degree of change. In the case of approximate average of Cu value, a low CV implies
143 elemental concentrations changing slightly along the borehole. In other words, it means more homogeneous
144 mineralization. Therefore, the fractal dimensions of mineralization are inversely related to CV. Figure 7
145 shows the regression line existing between fractal dimensions and CV. The squared correlation coefficient
146 R^2 is 0.84.

147 On the other hand, Figure 8A shows that the vertical distribution of Cu in ZK1901 exhibits a
148 multimodal distribution, which is caused by different wall rocks containing a different Cu content. The
149 explanation is that the distribution is the sum of several other distributions; therefore, the final density
150 distribution can become multimodal, particularly when the parent distributions characterize well-defined
151 source materials with different mean or modal values (Allègre and Lewin, 1995). Figure 8C illustrates three
152 regression lines existing in a log-log plot of cumulative number versus Cu values, which could be caused

153 by a multimodal distribution.

154 *4.4. Hurst Exponents*

155 The results obtained by Hurst exponents using R/S for 10 mineralized boreholes are shown in Fig.9
156 and listed in the last two columns of Table 2. The values of Hurst exponents range from 0.62 to 0.91, all
157 greater than 0.5, indicating persistent phenomena and better continuity of mineralization. The Hurst
158 exponent for the non-mineralized borehole Zk1901 is 0.87(Fig. 8D), and is also greater than 0.5 owing to
159 the homogeneous distribution of Cu in wall rocks.

160 **5. Conclusions**

161 The continuity of mineralization is a key issue in potential mineral resources assessment for a given
162 deposit. It can be recognized by characterizing the vertical distribution of geochemical concentration values
163 in borehole datasets. In this paper, three fractal dimensions, including box dimension, power-law frequency
164 and Hurst exponent, are used to investigate the irregularity and the continuity of Cu mineralization. The
165 following results are obtained:

166 (1) The vertical distribution of Cu values in mineralized and non-mineralized boreholes show
167 self-similarity with box dimensions ranging from 1.28 to 1.37. The box dimensions for mineralized
168 boreholes are greater than that of Cu values in non-mineralized borehole, indicating that the mineralization
169 process makes the distribution of Cu values more irregular.

170 (2) The vertical distribution of Cu values in mineralized and non-mineralized boreholes has different
171 characteristics: the former satisfies a positive skewed distribution and exhibits bifractal; while the latter
172 satisfies a multimodal distribution.

173 (3) Hurst exponents for mineralized boreholes are about 0.8, indicating that Qulong has a good
174 continuous mineralization.

175 **Acknowledgements**

176 The authors would like to thank two anonymous *Journal of Geochemical Exploration* referees for
177 their critical reviews of the manuscript and their constructive comments, as well as Reijo Salminen,
178 associate editor of *Journal of Geochemical Exploration*, for constructive suggestions. This research
179 was financially jointly supported by Chinese National Foundation of Science Projects ‘‘Distinguished
180 Young Researcher Grant’’ (40525009) and Strategic Research project (40638041).

181 **References**

- 182 Agterberg, F. P., 1993. Calculation of the variance of mean values for blocks in regional resource evaluation
183 studies: *Nonrenewable Resources* 2, 312-324.
- 184 Ahrens, L.H., 1954. The lognormal distribution of the elements (a fundamental law of geochemistry and its
185 subsidiary), *Geochim. Cosmochim. Acta* 5, 49-73.
- 186 Ahrens, L.H., 1963b. Lognormal-type distributions in igneous rocks-V, *Geochim. Cosmochim. Acta* 27,
187 877-890.
- 188 Ahrens, L.H., 1966. Element distributions in specific igneous rocks-VIII, *Geochim. Cosmochim. Acta* 30,
189 109-122.
- 190 Ahrens, L.H., 1957, 1957. Lognormal-type distributions-III, *Geochim. Cosmochim. Acta* 11, 205-212.
- 191 Ahrens, L.H., 1963a. Lognormal, 1963a. Lognormal-type distributions in igneous rocks-IV, *Geochim.*
192 *Cosmochim. Acta* 27, 333-343.
- 193 Allègre, C.L. and Lewin, E., 1995. Scale law Scaling laws and geochemical distributions. *Earth and*
194 *Planetary Science Letters* 132, 1-13.
- 195 Cheng, Q., 1995. The perimeter-area fractal model and its application to geology: *Math. Geol.* 27, 69-82.
- 196 Cheng, Q., Agterberg, F. P., and Ballantyne, S. B., 1994. The separation of geochemical anomalies from

- 197 background by fractal methods, *J. Geochem. Explor.* 51, 109-130.
- 198 Cheng, Q., Xu, Y., and Grunsky, E., 2000. Multifractal power spectrum-area method for geochemical
199 anomaly separation. *Natural Resources Research* 9, 43-51.
- 200 Hurst, H.E. 1951. Long-Term Storage Capacity of Reservoirs. *Transactions of the American Society of*
201 *Civil Engineers* .116, 770-808.
- 202 Kenneth,F., 1997. *Techniques in Fractal Geometry*. John Willey and Sons.
- 203 Li, C., Xu,Y., Xu, Y., Jiang, X., 1994. The fractal model of mineral deposits. *Geology of Zhejiang* 10, 25,
204 25-32 (In Chinese with English Abstract).
- 205 Mandelbrot, B. B., 1983.*The fractal geometry of nature*: W. H. Freeman and Company, New York (updated
206 and augmented edition).468pp.
- 207 Mandelbrot, B.B, and Wallis, J.R., 1969. Some long-run properties of geophysical records. *Water*
208 *Resource Research* 5, 321-340.
- 209 Monecke, T., Gemmel, J.B., Monecke, J., 2001. Fractal distributions of veins in drill core from the Hellyer
210 VHMS deposit, Australia: constraints on the origin and evolution of the mineralising system, *Miner.*
211 *Depos.* 36, 406-415.
- 212 Richardson, W.A., 1923. The frequency distribution of igneous rocks. Part II: the laws of distribution in
213 relation to petrogenetic theories, *Mineral. Mag.* 20, 1-4.
- 214 Rui, Z., Hou, Z., Qu, X., et al., 2003. Metallogenic Epoch of Gangdese Prophyry Copper Belt and Uplift
215 of Qinghai-Tibet Plateau. *Mineral Deposit* 22, 217-225 (In Chinese with English Abstract)
- 216 Sanderson, D. J., Roberts, S., Gumiel, P., 1994. A Fractal relationship between vein thickness and gold
217 grade in drill core from La Codosera, Spain, *Economic Geology* 89, 168-173.
- 218 Shi, J. and Wang, C., 1998. Fractal analysis of gold deposits in China: implication for giant deposit

- 219 exploration. *Earth Science-Journal of China University of Geosciences* 23, 616-618 (In Chinese with
220 English Abstract).
- 221 Turcotte, D.L., 1996. *Fractals and Chaos in Geophysics*. 2nd ed. Cambridge UK: Cambridge University
222 Press. pp.81-99.
- 223 Turcotte, D.L., 2002. Fractals in petrology. *Lithos* 65, 261-271.
- 224 Wang, Z., Cheng, Q., Cao, L. et al., 2006. Fractal modeling of the microstructure property of quartz
225 mylonite during deformation process. *Math. Geol.* 39, 53-68.
- 226 Wang, Z., Cheng, Q., Xu, D. Dong, Y., 2008. Fractal Modeling of Sphalerite Banding in Jinding Pb-Zn
227 Deposit, Yunnan, Southwestern China, *Journal of China University of Geosciences*, 19, 77-84.
- 228 Zheng, Y., Wang, B., Fan, Z., et al., 2002. Analysis of Tectonic Evolution in the Eastern Section of
229 Gangdise Mountains, Tibet and Metallogenic Potentialities of Copper Gold Polymetal. *Geological
230 Science and Technology Information* 21, 55-60 (In Chinese with English Abstract)

231 **Figure and Table Captions**

- 232 Fig.1. Simplified geological map of Qulong Copper Deposit
- 233 Fig.2. The profile of the eighth exploring line
- 234 Fig.3. Plots of Cu values for 10 mineralized boreholes
- 235 Fig.4. The histograms of Cu values from 10 mineralized boreholes
- 236 Fig.5. Log-log plots of number versus box size for 10 mineralized Cu values (Logs base 10)
- 237 Fig.6. Log-log plots of cumulative number versus Cu grade 10 mineralized boreholes (Logs base $e=2.732$)
- 238 Fig.7. Plot of fractal dimensions for mineralization versus coefficient of variation along with regression line
- 239 Fig.8. (A) is the histogram of Zk1901 Cu grade; (B) log-log plots of number versus box size for Cu values
240 (Logs base 10); (C) is power-law frequency for non-mineralized borehole Zk1901 and (D) is log-log plot of

- 241 R/S versus number for non-mineralized borehole (Logs base 10)
- 242 Fig.9.Log-log plots of R/S versus number for 10 mineralized boreholes (Logs base 10)
- 243 Table 1.The basic information and statistical properties for 10 mineralized boreholes and 1 non-mineralized
- 244 borehole from Qulong Copper Deposit
- 245 Table 2.The fractal dimension of Cu values from Qulong copper deposit

ACCEPTED MANUSCRIPT

Table 1 .The basic information and statistical properties of 10 mineralized boreholes and 1 non-mineralized borehole from Qulong Copper Deposit

NO.	X	Y	Number of Samples	Elevation(m)	Cu Max (%)	Cu Min (%)	Cu Average (%)	Std.	CV
ZK001	64.20	79.30	147	5085	1.79	0.14	0.48	0.27	0.56
ZK002	64.24	79.10	104	5210	1.21	0.02	0.34	0.15	0.44
ZK003	64.11	79.80	239	5390	2.20	0.07	0.45	0.28	0.62
ZK004	64.15	78.63	63	5215	1.01	0.03	0.27	0.16	0.59
ZK801	64.55	79.30	273	5085	1.58	0.02	0.50	0.21	0.42
ZK802	64.55	79.70	243	5080	1.06	0.20	0.51	0.11	0.22
ZK803	64.55	79.90	261	5115	1.07	0.22	0.45	0.12	0.27
ZK1601	64.95	79.30	206	5160	0.94	0.26	0.49	0.11	0.22
ZK1101	63.60	79.83	175	5375	1.29	0.10	0.37	0.16	0.43
ZK701	63.73	79.32	146	5370	1.00	0.09	0.40	0.16	0.40
Zk1901	65.50	80.5	85	5230	0.093	0.003	0.037	0.027	0.72

Note: Std. is the standard deviation, and CV is standard coefficient of variation

Table 2. The fractal dimensions of Cu in Qulong Copper Deposit

Borehole	Box dimensions		Power-law frequency					Hurst exponent	
	dimensions	R ²	dimension 1	R ²	break point	dimension 2	R ²	Hurst	R ²
ZK001	1.30	1.00	0.22	1.00	0.33	2.74	0.97	0.82	0.97
ZK002	1.28	1.00	0.1	0.64	0.33	3.75	0.97	0.75	0.91
ZK003	1.38	1.00	0.23	0.95	0.33	2.71	0.99	0.77	0.99
ZK004	1.37	1.00	0.24	0.85	0.24	2.83	0.98	0.80	0.95
ZK801	1.35	1.00	0.11	0.6	0.37	3.60	0.99	0.62	0.95
ZK802	1.37	1.00	0.3	0.64	0.45	4.25	0.99	0.91	0.98
ZK803	1.34	1.00	0.32	0.92	0.37	4.89	0.99	0.88	0.96
ZK1601	1.37	1.00	0.65	0.96	0.45	5.79	0.96	0.83	0.96
ZK1101	1.34	1.00	0.22	0.81	0.33	3.38	0.99	0.71	0.95
ZK701	1.32	1.00	0.21	0.74	0.33	3.92	0.96	0.73	0.97
ZK1901	1.28	0.99	0.2	0.97	0.22	1.67	0.96	0.87	0.96

Note: Dimension 1 denotes the negative slope of the upper regression line in power-law frequency, and dimension 2 denotes the negative slope of the lower regression line in power-law frequency.

Figure 1

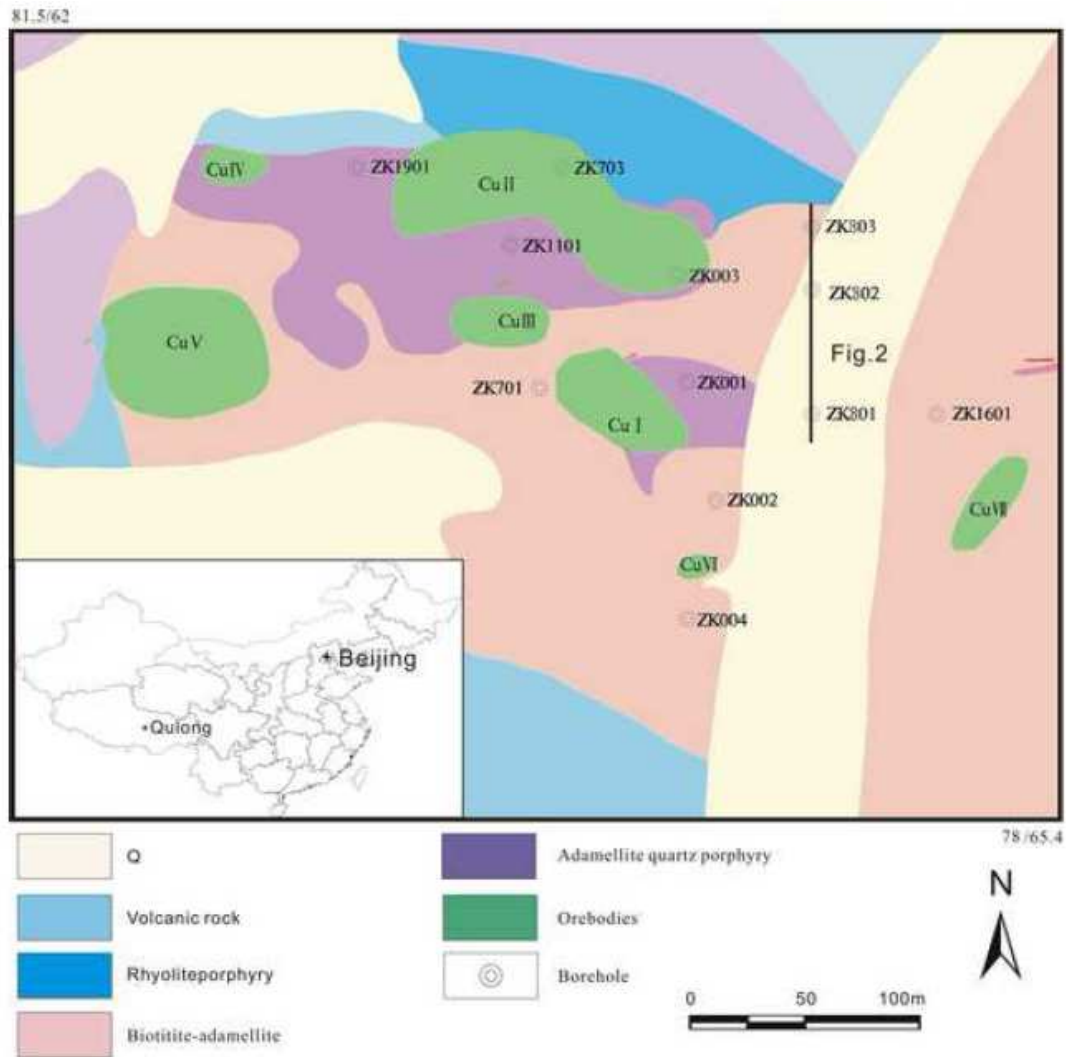


Figure 2

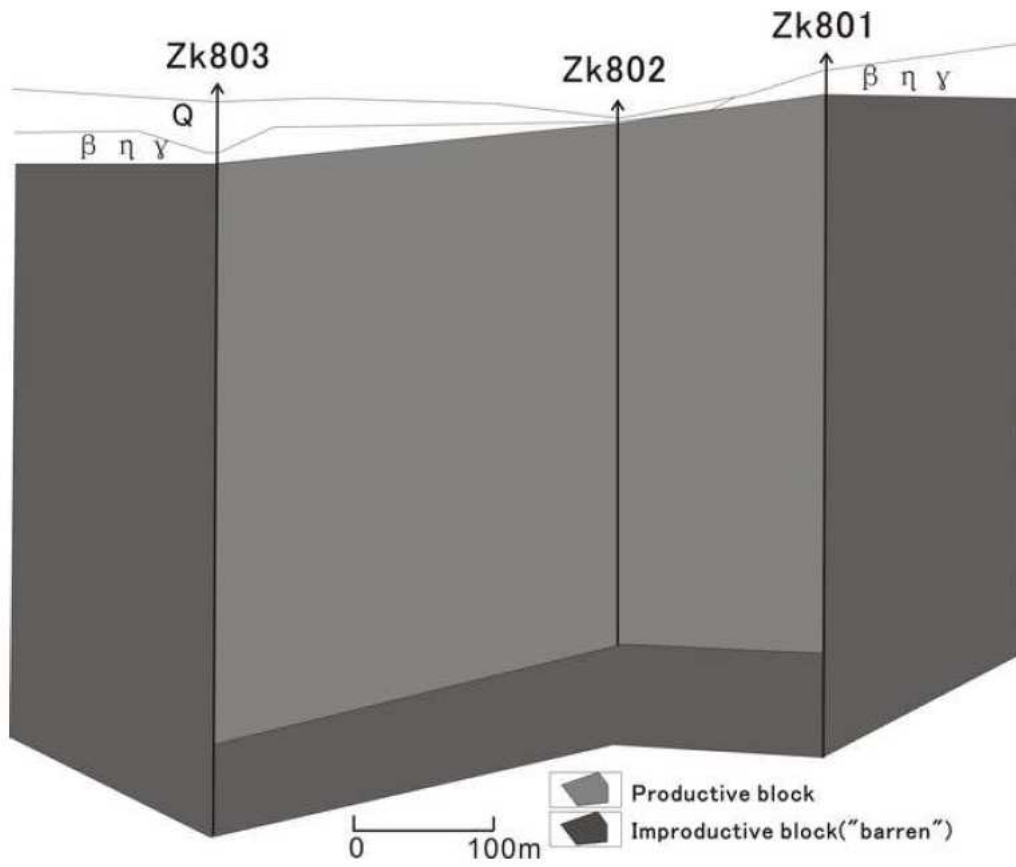
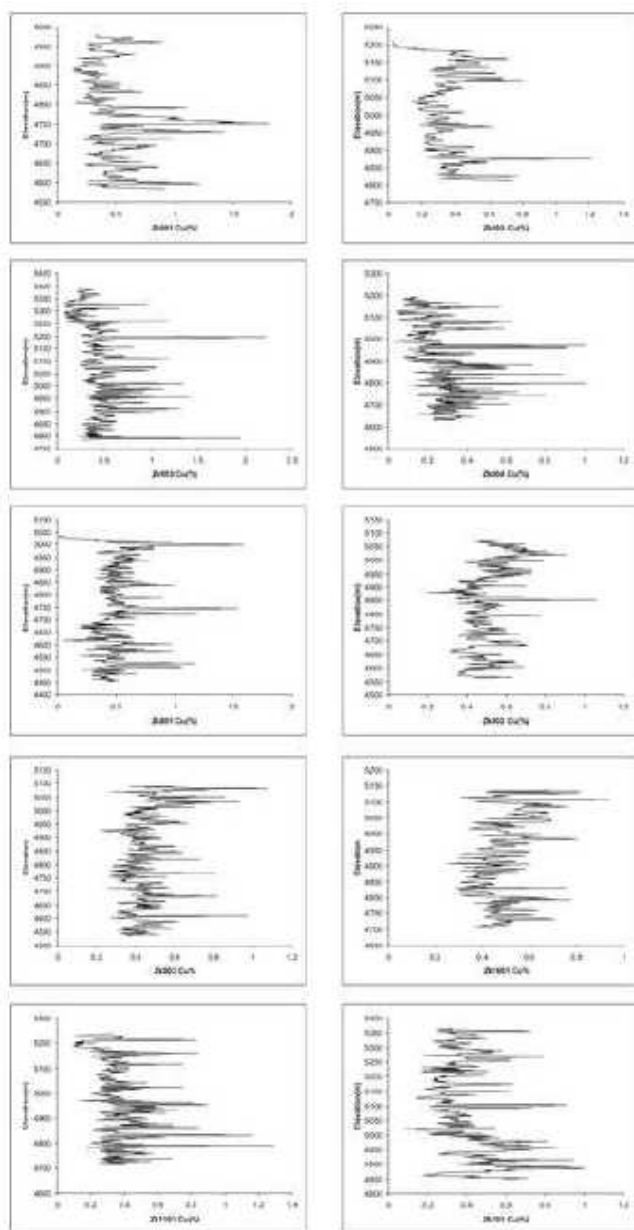


Figure 3



SCRIPT

Figure 4

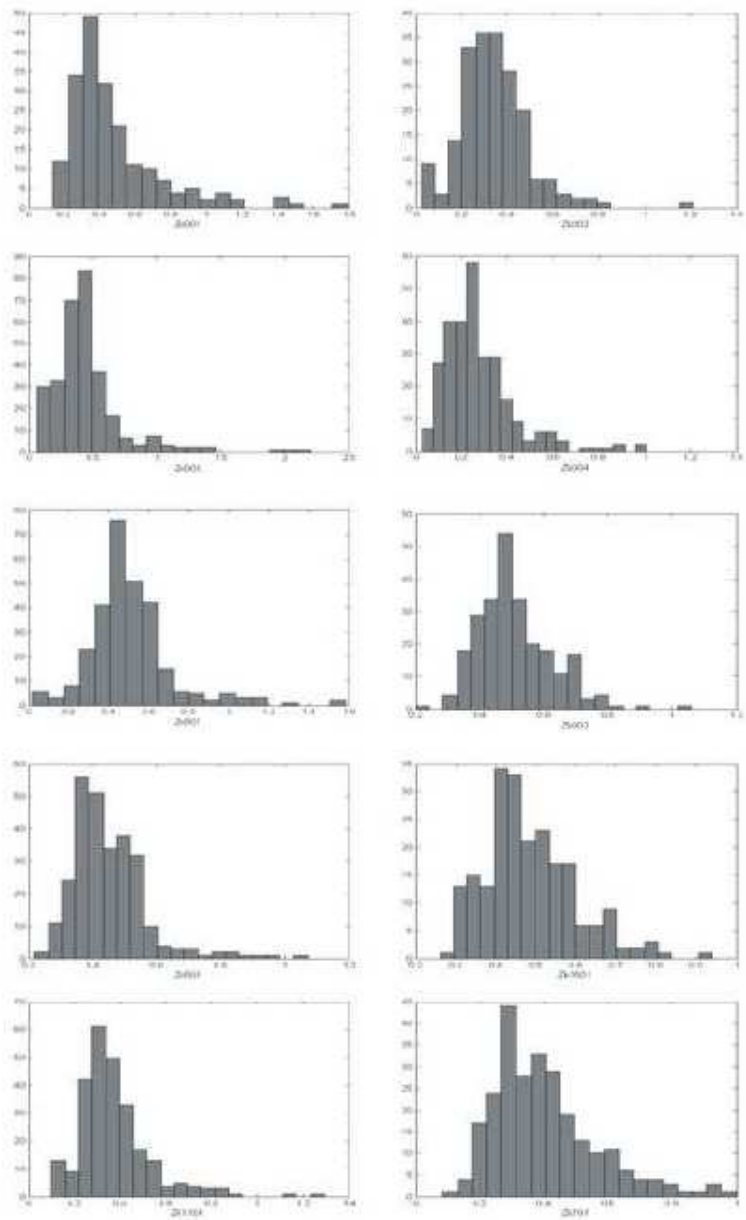


Figure 5

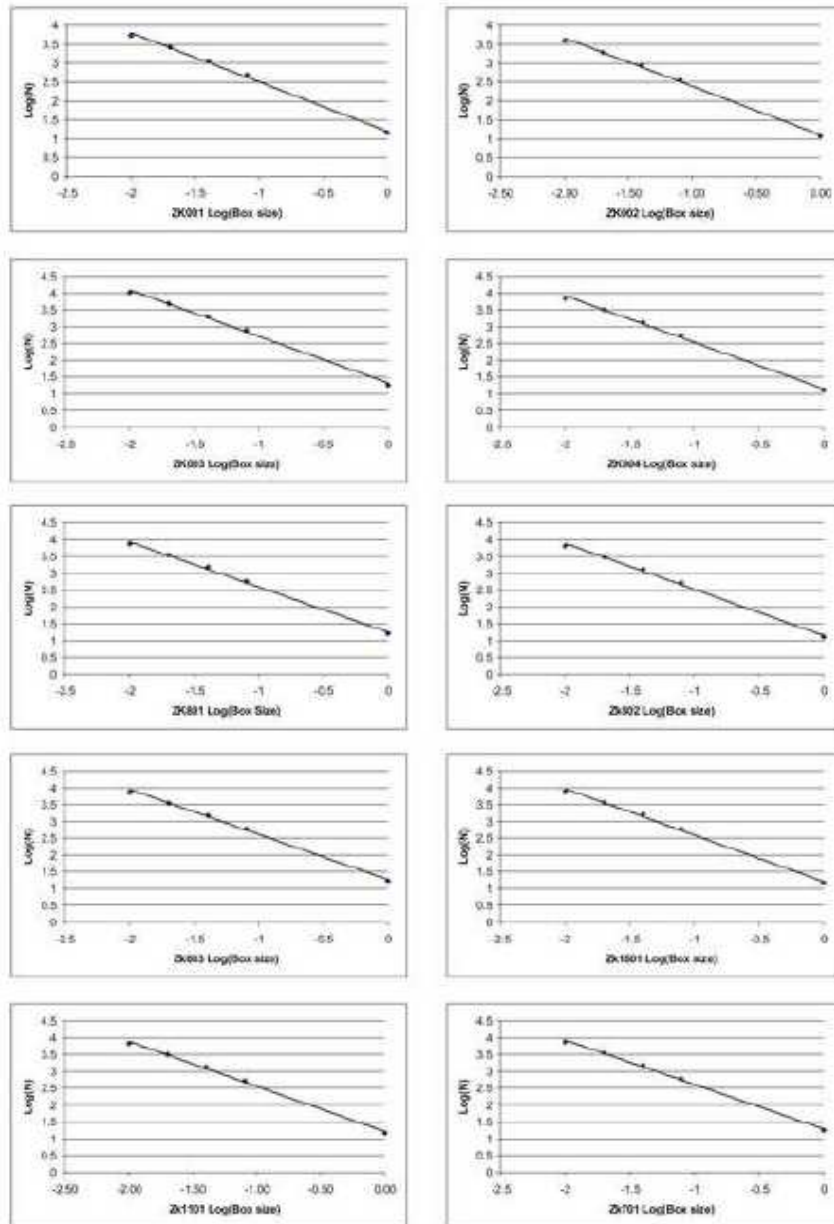


Figure 6

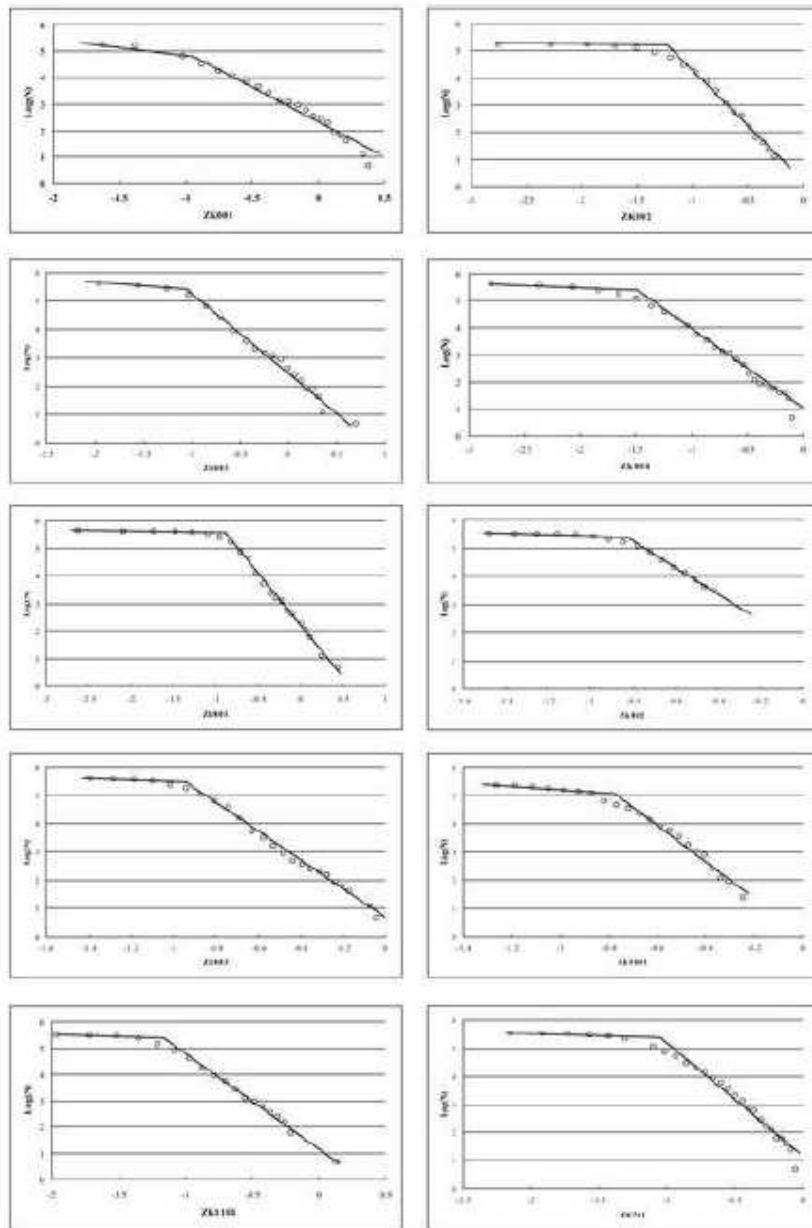
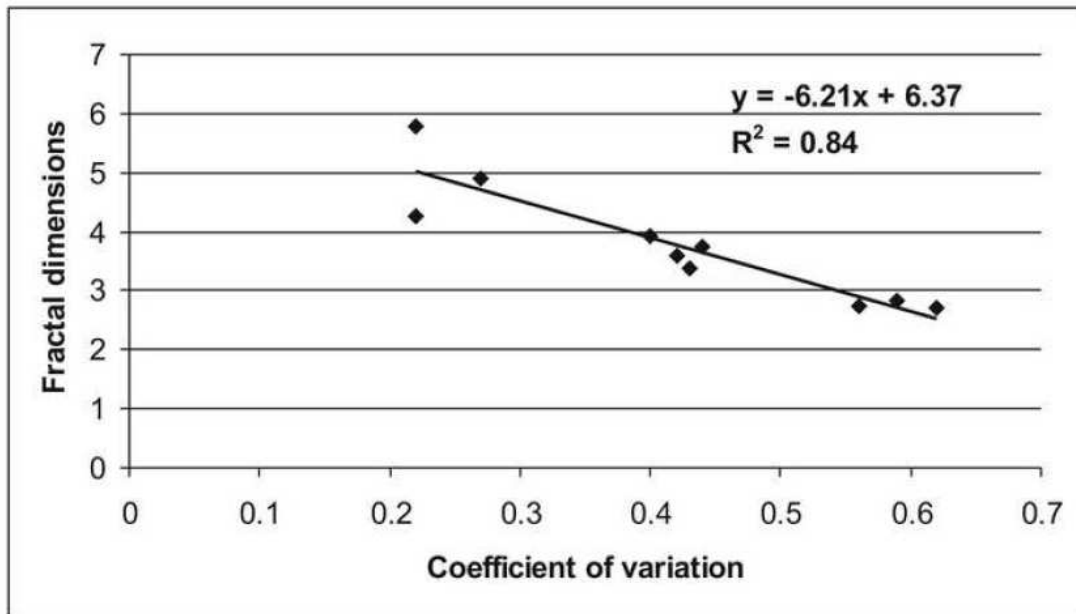
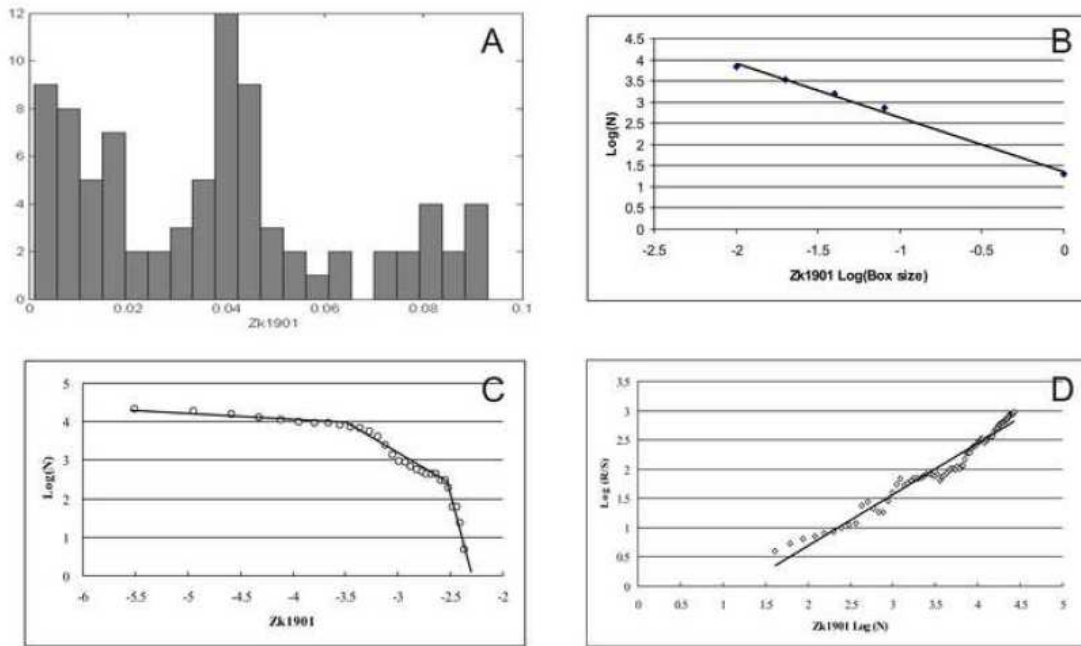


Figure 7



ACCEPTED

Figure 8



ACCEPTED

Figure 9

